PASJ: Publ. Astron. Soc. Japan **57**, L7–L10, 2005 June 25

Discovery of a Fifth Image of the Large Separation Gravitationally Lensed Quasar SDSS J1004+4112 *

Naohisa INADA,[1] Masamune OGURI,[2,3] Charles R. KEETON,[4] Daniel J. EISENSTEIN,[5]
Francisco J. CASTANDER,[6] Kuenley CHIU,[7] Patrick B. HALL,[8] Joseph F. HENNAWI,[9] David E. JOHNSTON,[2]
Bartosz PINDOR,[10] Gordon T. RICHARDS,[2] Hans-Walter RIX,[11] Donald P. SCHNEIDER,[12] and Wei ZHENG[7]
[1]*Institute of Astronomy, Faculty of Science, The University of Tokyo, 2-21-1 Osawa, Mitaka, Tokyo 181-0015*
[2]*Princeton University Observatory, Peyton Hall, Princeton, NJ 08544, USA*
[3]*Department of Physics, School of Science, The University of Tokyo, 7-3-1 Hongo, Bunkyo-ku, Tokyo 113-0033*
[4]*Department of Physics and Astronomy, Rutgers University, 136 Frelinghuysen Road, Piscataway, NJ 08854, USA*
[5]*Steward Observatory, University of Arizona, 933 North Cherry Avenue, Tucson, AZ 85721, USA*
[6]*Institut d'Estudis Espacials de Catalunya/CSIC, Gran Capita 2-4, E-08034 Barcelona, Spain*
[7]*Department of Physics and Astronomy, The Johns Hopkins University, 3701 San Martin Drive, Baltimore, MD 21218, USA*
[8]*Department of Physics and Astronomy, York University, 4700 Keele Street, Toronto, Ontario, M3J 1P3, Canada*
[9]*Department of Astronomy, University of California at Berkeley, 601 Campbell Hall, Berkeley, CA 94720, USA*
[10]*Department of Astronomy, University of Toronto, 60 St.George Street, Toronto, Ontario M5S 3H8, Canada*
[11]*Max-Planck-Institut für Astronomie, Königstuhl 17, Heidelberg, D-69117, Germany*
[12]*Department of Astronomy and Astrophysics, Pennsylvania State University, 525 Davey Laboratory, University Park, PA 16802, USA*

(Received 2004 October 27; accepted 2005 March 14)

Abstract

We report on the discovery of a fifth lensed image in the large separation lensed quasar system SDSS J1004+4112. A faint point source located 0.″2 from the center of the brightest galaxy in the lensing cluster was detected in images taken with the Advanced Camera for Surveys (ACS) and the Near Infrared Camera and Multi-Object Spectrometer (NICMOS) on the Hubble Space Telescope. The flux ratio between the point source and the brightest lensed component in the ACS image is similar to that in the NICMOS image. The location and brightness of the point source are consistent with lens model predictions for a lensed image. We therefore conclude that the point source is likely to be a fifth lensed image of the source quasar. In addition, the NICMOS image reveals the lensed host galaxy of the source quasar, which can strongly constrain the structure of the lensing critical curves, and thereby the mass distribution of the lensing cluster.

Key words: galaxies: quasars: individual (SDSS J1004+4112) — galaxies: structure — gravitational lensing

1. Introduction

Gravitational lensing is a unique tool for exploring the distribution of matter, particularly that of dark matter. The recently discovered largest separation lensed quasar, SDSS J1004+4112 (Inada et al. 2003; Oguri et al. 2004), has opened a new window for probing dark-matter distributions in the universe. The quasar was discovered in the Sloan Digital Sky Survey (SDSS; York et al. 2000; Abazajian et al. 2004), and the lensing hypothesis was confirmed by subsequent observations with the Subaru 8.2-m telescope and the Keck telescope. The system consists of four lensed quasar components (i' = 18.5, 18.9, 19.4, and 20.1) at z = 1.734; the maximum separation angle between the lensed images is 14.″62. The lensing object must be a massive object, such as a cluster of galaxies, to produce such a large image separation; indeed, we have identified a z = 0.68 cluster centered among the four lensed images. The discovery of a single, cluster-size lensed quasar among the current SDSS quasars is consistent with the theoretical expectation of lensing based on the cold dark-matter model (Oguri et al. 2004; Oguri, Keeton 2004).

SDSS J1004+4112 is unique in the sense that: 1) quadruple images place robust constraints on the innermost region of the lensing cluster, and 2) the lensing cluster is a *strong lensing selected* cluster of galaxies. These features indicate that the mass modeling of this lens system may offer valuable information on the structure of clusters of galaxies. The first attempt at modeling the system with various parametric models revealed the elongated and complicated mass distribution of the lensing cluster (Oguri et al. 2004). Williams and Saha (2004) recently studied this system using a free-form reconstruction technique, and reached similar conclusions. However, important degeneracies between different models remain, and further follow-up observations are required to determine the mass distribution more precisely.

Observations using the Hubble Space Telescope (HST) can offer such new data. In particular, high-resolution HST images could be quite effective at detecting lensed images of the quasar host galaxy, arc or arclet images of other lensed sources,

* Based on observations with the NASA/ESA Hubble Space Telescope, obtained at the Space Telescope Science Institute, which is operated by the Association of Universities for Research in Astronomy, Inc., under NASA contract NAS 5-26555. These observations are associated with HST program 9744.

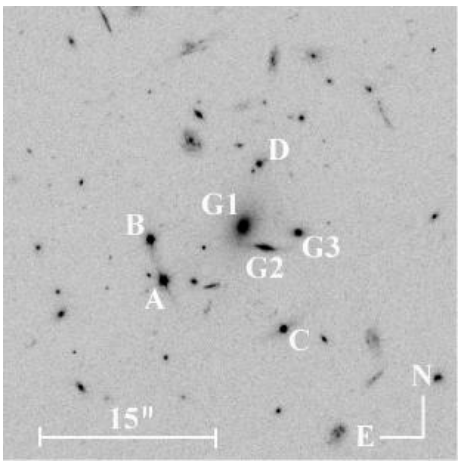

Fig. 1. $40'' \times 40''$ subsection of the median combined ACS image of SDSS J1004+4112. The four quasar images are labeled A–D. The galaxies of the lensing cluster labeled G1–G3 have redshifts of 0.680, 0.675, and 0.675, respectively. The pixel scale is approximately $0\farcs05\,\mathrm{pixel}^{-1}$.

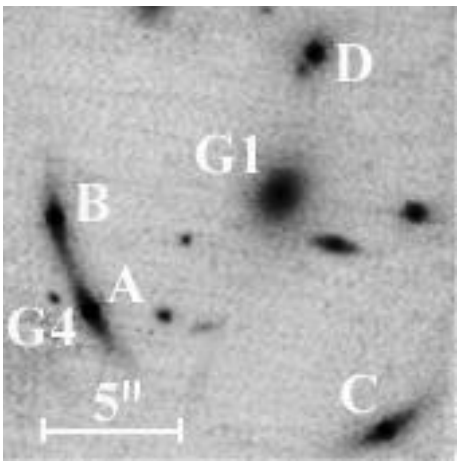

Fig. 2. Combined NICMOS image of SDSS J1004+4112. The pixel scale is approximately $0\farcs075\,\mathrm{pixel}^{-1}$. The lensed host galaxy is seen more prominently in this NICMOS image than in the ACS image. In addition, we can see G4 near component A.

and perhaps a central or "odd" image of the lensed quasar system, which would be expected theoretically (e.g., Burke 1981; Rusin 2002). A central image is especially useful for providing tight constraints on the central mass distribution of the lensing object. This was indeed demonstrated by the first discovery of a central image in a lensed quasar system; Winn, Rusin, and Kochanek (2004) showed that the central image of PMN J1632−0033 requires $\beta = 1.91 \pm 0.02$ (2σ confidence) when a power-law density profile $\rho(r) \propto r^{-\beta}$ is assumed. Possible central images have also been identified in lensed arc systems, such as CL 0024+1654 (Colley et al. 1996), MS 2137.3−2353 (Gavazzi et al. 2003), and A1689 (Broadhurst et al. 2005). They also provide important constraints on mass models (see e.g., Gavazzi et al. 2003).

In this letter, we present the identification of a fifth image of the lensed quasar with the Advanced Camera for Surveys (ACS; Clampin et al. 2000) as well as the Near Infrared Camera and Multi-Object Spectrometer (NICMOS; Thompson 1992) installed on the HST. In addition, we report on an unambiguous detection of the lensed host galaxy in the NICMOS image.

2. The ACS Observation

An ACS observation (with the Wide Field Channel) in the F814W filter ($\approx I$-band) was conducted on 2004 April 28, under the program "HST Imaging of Gravitational Lenses" (GO-9744, PI C. Kochanek). The observation consisted of five dithered exposures taken in the ACCUM mode. The total exposure time was 405 sec. Reduced (drizzled and calibrated) images were extracted using the CALACS pipeline (Hack 1999), which includes the PyDrizzle algorithm. We further rejected cosmic rays using the L.A.COSMIC package (van Dokkum 2001) in the drizzled image. A $40'' \times 40''$ subsection of the median of the five dithered images is shown in figure 1. Following figure 9 of Oguri et al. (2004), the four lensed components are denoted as "A–D", and three central bright galaxies of the lensing cluster are denoted as "G1–G3". The redshifts of galaxies G1–G3 are 0.680, 0.675, and 0.675, respectively (Oguri et al. 2004). The relative positions of components A–D were calculated by a single Gaussian fit, and the flux ratios of components A–D were estimated by fitting the PSF stars produced by the Tiny Tim software (version 6.1a; Krist, Hook 2003), in the drizzled (and cosmic-ray rejected) image. The PSF of a quasar was constructed with an $\alpha_\nu = -0.5$ power-law spectrum in the F814W wavelength region (corresponding to ~ 3000 Å in the rest frame). The relative positions derived from the ACS (F814W) are consistent with those derived from the Subaru i'-band image (Oguri et al. 2004) within $\sim 5\sigma$. The four components are all unsaturated, and the AB magnitude of component A in the F814W filter is estimated to be 18.4. The position of component G1 was extracted by the Source Extractor algorithm (Bertin, Arnouts 1996). The results are summarized in table 1.

3. The NICMOS Observation

The NICMOS imaging observation was also conducted under the same HST program on 2004 October 9. The observation consists of four dithered exposures taken in the

Table 1. Relative positions and flux ratios of SDSS J1004+4112 in the HST ACS image.

Object	x (arcsec)*	y (arcsec)*	Flux ratio†
A	0.0000 ± 0.001	0.0000 ± 0.001	1.000
B	-1.317 ± 0.002	3.532 ± 0.002	0.732
C	11.039 ± 0.002	-4.492 ± 0.002	0.346
D	8.399 ± 0.004	9.707 ± 0.004	0.207
E	7.197 ± 0.009	4.603 ± 0.009	0.003
G1	7.114 ± 0.030	4.409 ± 0.030	⋯

* The positive directions of x and y are defined by west and north, respectively.

† Errors of fitting by quasar PSFs are about 10%. The error of component E might be much larger due to the over-subtraction of G1.

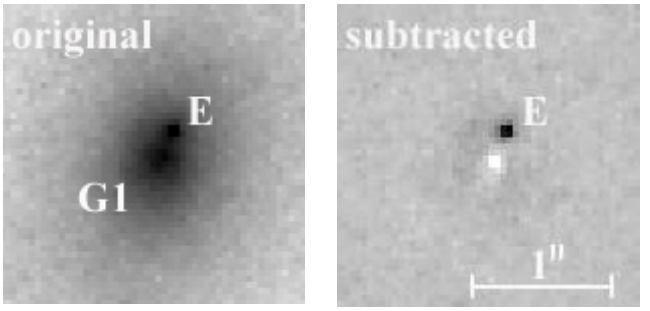

Fig. 3. Left: ACS image of central galaxy G1. Right: ACS image after subtracting galaxy G1. The residual image clearly shows a stellar object near the center of G1.

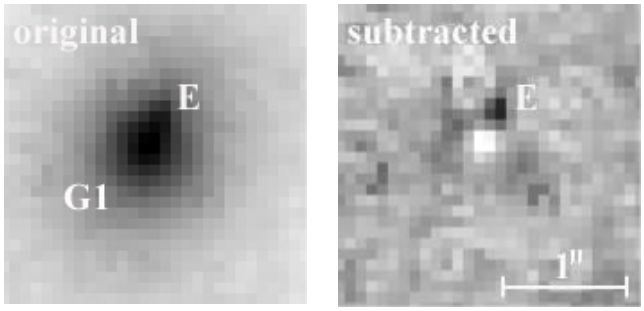

Fig. 4. Left: NICMOS image of central galaxy G1. Right: NICMOS image after subtracting galaxy G1. The stellar object near the center of G1 can also be seen in the NICMOS image.

MULTIACCUM mode, using the F160W filter ($\approx H$-band). The exposure time was 640 sec for two of the exposures and 704 sec for the other two. The calibration was extracted by the CALNICA pipeline, and the central bad columns of each dithered image were corrected by linear interpolation. The combined image is shown in figure 2. First, we confirm a galaxy near component A (marked as G4 in figure 2), which may host the star, or stars, responsible for microlensing of the broad emission line region (Richards et al. 2004). In addition, extended emission is clearly seen around components A, B, and C. Although such extensions are also seen in the ACS images (see figure 1), their existence is much more robust in the NICMOS image. The facts that these extensions are obvious in the F160W (near-infrared) image and faint in the F814W (optical) image, and that the distortions agree with the theoretical critical curves (see figure 17 of Oguri et al. 2004), demonstrate that the extended flux is due to the lensed host galaxy of the source quasar. These images provide many new constraints on lens models that will significantly improve our ability to determine the mass distribution of the lensing cluster. They do make lens modeling more computationally intensive (because one must account for the intrinsic shape of the host galaxy, and also for the effects of the point spread function), so we defer detailed modeling of the arcs to a subsequent paper.

4. Fifth Lensed Image

Of interest is the existence of a point source near the center of G1. The left panel in figure 3 shows the ACS image of galaxy G1; what appears to be an unresolved source is clearly seen approximately $0\farcs2$ northwest of the center of G1. *This feature is neither a bad pixel nor a cosmic ray*; the source is seen in all dithered images. The right panel in figure 3 displays the image after subtracting the signal from G1 (modeled with the GALFIT package of Peng et al. 2002). Due to the existence of an unresolved source near the center of G1 (the peak flux of this unresolved source is almost same as that of G1), G1 was slightly over-subtracted. However, we can see a new source, labeled E, in the subtracted image. This object is classified as a point source by the Source Extractor algorithm. The position and brightness of E, based on a single Gaussian fit to the data, are given in table 1.

We also find component E in the NICMOS image; the left panel in figure 4 is a NICMOS image of galaxy G1. We subtracted the signal from G1 using the GALFIT package, which is shown in the right panel of figure 4. We confirmed component E in the subtracted image, although G1 was slightly over-subtracted as in the ACS image. Measuring the flux of component E with a single Gaussian fit, we found that the flux ratios between E and A (E/A) in the ACS and NICMOS images are 0.003 and 0.004, respectively. This remarkable agreement of the flux ratios supports the idea that the point source is a fifth image of the lensed quasar.

To test this hypothesis, we have refined the lens models presented in Oguri et al. (2004) using the more precise HST data. The models consist of a singular isothermal ellipsoid mass distribution for galaxy G1, and an NFW (Navarro et al. 1997) elliptical potential for the cluster. We demanded that the models reproduced the relative positions and brightnesses of components A–D (and the relative position of G1), as well

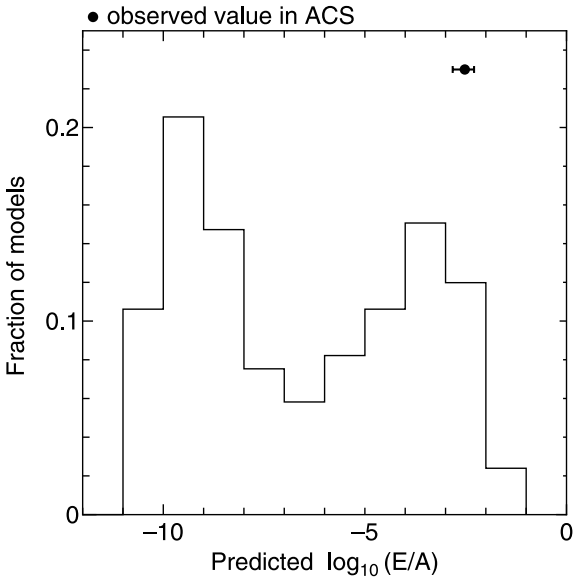

Fig. 5. Frequency (fraction of models) of the predicted flux ratio of E/A from two component (central galaxy + cluster component) lens models. The models are constrained by the observed positions and brightnesses of components A–D (and the observed position of G1), and the position of component E. Although we assume that the scale radius of the NFW component is $40\farcs0$, the results are insensitive to the particular value. The gray filled circle represents the observed value of E/A (in ACS) with 50% error.

as the position of component E; we did not use the brightness of E as a constraint, because we wanted to see what the models predict. Adopting the same approach as Oguri et al. (2004), we used the *lensmodel* software (Keeton 2001) for Monte Carlo sampling of the parameter space. There is a wide range of models consistent with the data, indicating that it is not difficult to produce a 5-image lens matching the configuration of components A–E, and that significant model degeneracies remain. More interesting are the model predictions for the flux ratio between the fifth image and component A, shown in figure 5. The predictions span a remarkable nine orders of magnitude, from $E/A \sim 0.1$ down to $E/A \sim 10^{-10}$, but a significant fraction predicts E/A in the range of 0.001–0.01, consistent with the observed value. In other words, there are (many) reasonable models that can fit all of the HST data under the hypothesis that E is a fifth image; conversely, the observed properties of E are highly compatible with that hypothesis.

Given the enormous range of model predictions for the brightness of E, it appears that the observed brightness offers strong constraints on the models. We caution that one must be careful in using the brightness of E as a constraint, because its measured flux could be contaminated by improper subtraction of the galaxy, or by such physical effects as microlensing and extinction. Nevertheless, the range of the predictions is so large that even conservative estimates of systematic uncertainties should still yield very interesting results. As an example, to test the ability of E to constrain the central density profile of G1, we switch from an isothermal model to a more general power-law density profile, $\rho(r) \propto r^{-\beta}$, for the galaxy (for computational simplicity, we now assume that the *potential*, rather than the density, has elliptical symmetry). We have found that there is a wide range of models with $1.6 \leq \beta \leq 2.0$ that predicts $0.001 \lesssim E/A \lesssim 0.01$. By contrast, all of the models that we examined with $\beta \geq 2.1$ predict $E/A \lesssim 10^{-10}$, which grossly contradicts even a conservative reading of the data. In other words, the observed properties of E imply that the galaxy mass distribution cannot be steeper than isothermal (i.e., $\beta \leq 2$). This upper bound is similar to that found by Winn, Rusin, and Kochanek (2004) from the central image in PMN J1632−0033 (specifically, they found $\beta = 1.91 \pm 0.02$). However, SDSS J1004+4112 differs from PMN J1632−0033 in that we do not obtain any *lower* bound on β, at least over the range $1.6 \leq \beta \leq 2.0$, which we have explored so far. Apparently the complexity of the SDSS J1004+4112 lens potential, with a cluster in addition to the galaxy, prevents a unique measurement of the value of β. Nevertheless, it is clear that component E provides important new constraints on the mass distribution of this interesting lens system.

5. Summary

We have presented HST ACS and NICMOS images of SDSS J1004+4112, which reveal a fifth lensed image of the lensed quasar core. The fifth lensed image offers a unique probe of the mass distribution of the cluster core. Deep spectroscopic observations of component E with large telescopes, such as the Subaru Telescope, offer the best prospect for the final confirmation that it is a lensed quasar image. In the NICMOS image, we also found unambiguous evidence of the lensed host galaxy of the source quasar. These extended images provide strong additional constraints on mass models of the lensing cluster, which are expected to break degeneracies seen in the modeling studies to date. A detailed analysis of lens models including the host galaxy images is underway and will be presented elsewhere.

A portion of this work was supported by NASA HST-GO-09744.20. N.I. and M.O. are supported by JSPS through JSPS Research Fellowship for Young Scientists.

Funding for the creation and distribution of the SDSS Archive has been provided by the Alfred P. Sloan Foundation, the Participating Institutions, the National Aeronautics and Space Administration, the National Science Foundation, the U.S. Department of Energy, the Japanese Monbukagakusho, and the Max Planck Society. The SDSS Web site is ⟨http://www.sdss.org/⟩.

The SDSS is managed by the Astrophysical Research Consortium (ARC) for the Participating Institutions. The Participating Institutions are The University of Chicago, Fermilab, the Institute for Advanced Study, the Japan Participation Group, The Johns Hopkins University, the Korean Scientist Group, Los Alamos National Laboratory, the Max-Planck-Institute for Astronomy (MPIA), the Max-Planck-Institute for Astrophysics (MPA), New Mexico State University, University of Pittsburgh, University of Portsmouth, Princeton University, the United States Naval Observatory, and the University of Washington.

References

Abazajian, K., et al. 2004, AJ, 128, 502
Bertin, E., & Arnouts, S. 1996, A&AS, 117, 393
Broadhurst, T., et al. 2005, ApJ, 621, 53
Burke, W. L. 1981, ApJ, 244, L1
Clampin, M., et al. 2000, Proc. SPIE, 4013, 344
Colley, W. N., Tyson, J. A., & Turner, E. L. 1996, ApJ, 461, L83
Gavazzi, R., Fort, B., Mellier, Y., Pelló, R., & Dantel-Fort, M. 2003, A&A, 403, 11
Hack, W. J. 1999, CALACS Operation and Implementation, Instrument Sci. Rep. ACS-99-03
Inada, N., et al. 2003, Nature, 426, 810
Keeton, C. R. 2001, astro-ph/0102340
Krist, J. E., & Hook, R. N. 2003, The Tiny Tim User's Guide, Version 6.1a (Baltimore: STScI)
Navarro, J. F., Frenk, C. S., & White, S. D. M. 1997, ApJ, 490, 493
Oguri, M., et al. 2004, ApJ, 605, 78
Oguri, M., & Keeton, C. R. 2004, ApJ, 610, 663
Peng, C. Y., Ho, L. C., Impey, C. D., & Rix, H.-W. 2002, AJ, 124, 266
Richards, G. T., et al. 2004, ApJ, 610, 679
Rusin, D. 2002, ApJ, 572, 705
Thompson, R. 1992, Space Sci. Rev., 61, 69
van Dokkum, P. G. 2001, PASP, 113, 1420
Williams, L. L. R., & Saha, P. 2004, AJ, 128, 2631
Winn, J. N., Rusin, D., & Kochanek, C. S. 2004, Nature, 427, 613
York, D. G., et al. 2000, AJ, 120, 1579